Iran Polym J (2017) 26:71–79
DOI 10.1007/s13726-016-0499-4

ORIGINAL PAPER

Expanded polystyrene foams containing ammonium polyphosphate and nano-zirconia with improved flame retardancy and mechanical properties

Zhengzhou Wang[1,2] · Shujian Jiang[1] · Haoyu Sun[1]

Received: 17 July 2016 / Accepted: 17 December 2016 / Published online: 29 December 2016
© Iran Polymer and Petrochemical Institute 2016

Abstract Expanded polystyrene (EPS) foams were flame retarded using ammonium polyphosphate (APP) and nano-zirconia (nano-ZrO_2) by means of phenolic resin as a binder. It is found that the incorporation of a small amount (5 phr) of nano-ZrO_2 into the APP flame-retarded EPS foams leads to 19% increase in flexural strength and 38% increase in compressive strength. Flame-retardant properties of the flame-retarded EPS foams were investigated by limiting oxygen index (LOI), UL-94 and cone calorimetry test (CCT). The LOI of the APP flame-retarded EPS foams in presence of nano-ZrO_2 is above 31%, and the UL 94 V-0 rating can be reached. The CCT test results indicate that the APP flame-retarded EPS foams containing nano-ZrO_2 have lower peak heat release rate, average effective heat of combustion and average specific extinction area. Moreover, thermal decomposition of the flame-retarded EPS foams was investigated by thermogravimetric analysis (TGA) and the TGA results illustrated clearly that the addition of nano-ZrO_2 into the APP flame-retarded EPS foams leads to an increase in the residual char yield. The reason for the increase is possibly because ZrO_2 may react during combustion process with pyrophosphoric acid produced from the thermal decomposition of APP to form zirconium pyrophosphate (ZrP_2O_7) confirmed by XRD studies of the char, which is helpful to improve the formation of the char. The XPS results showed that the ratio of oxidized carbons in the char increases with the presence of nano-ZrO_2.

Keywords Halogen-free flame retardation · Expanded polystyrene foams · Ammonium polyphosphate · Nano-zirconia

Introduction

Expanded polystyrene (EPS) foams due to their good thermal insulating properties, low density and low cost, are widely used in many fields such as building and transportation [1]. However, the EPS foams are easily flammable and set on fires quickly [2]. As a result, it is very necessary to improve the flame retardancy of EPS foams.

Nowadays, the flame retardation of EPS foams and extruded polystyrene (XPS) foams is mainly achieved in industry by halogen-containing flame retardants, i.e., hexabromocyclododecane (HBCD). HBCD is generally introduced into expandable polystyrene beads containing a homogeneously dispersed blowing agent (e.g., *n*-pentane) during the suspension polymerization of styrene monomers, and the EPS beads are prefoamed and molded into EPS foams. This method may be suitable for EPS foams with efficient halogen-containing flame retardants, because introduction of many flame retardants during styrene polymerization can very much affect properties of polystyrene (e.g., T_g) [3]. The use of halogen-containing flame retardants (i.e., HBCD) has led to some serious concerns about their toxicological and environmental impact [4, 5]. Therefore, halogen-free flame retardation for EPS foams is urgently needed.

The halogen-free flame retardation for EPS foams is usually carried out by treatment of EPS beads using binders

✉ Zhengzhou Wang
zwang@tongji.edu.cn

[1] School of Materials Science and Engineering, Tongji University, Shanghai 201804, People's Republic of China

[2] Key Laboratory of Advanced Civil Engineering Materials, Ministry of Education, Tongji University, Shanghai 201804, People's Republic of China

containing halogen-free flame retardants, then foamed and molded. The thermosetting phenolic resins are usually selected as binders because of their inherent fire resistance after curing and their good compatibility with EPS beads and inorganic fillers [6]. For example, Hong et al. [7] used ten parts of the mixture containing phenolic resin, aluminum hydroxide, boric acid and glass fiber, and one part of sodium dodecyl sulfate water solution to treat eight parts of EPS beads to produce composite EPS foam. It has been found that the composite foam can melt and retract and has no dripping when in contact with the flame.

In our previous work [8], two kinds of aluminum phosphinates, diethyl aluminum phosphinate (DEAP) and diisobutyl aluminum phosphinate (DIAP), or their combination with expandable graphite (EG) by means of phenolic resin binder were introduced into EPS foams, and the effect of ratio of aluminum phosphinates to EG on foam properties was investigated. The results showed that the limiting oxygen index (LOI) of the treated foams in presence of EG, DEAP and DIAP were 32.5, 29 and 27%, respectively, and EG was more efficient in improving flame retardancy of the foams compared to DEAP or DIAP. Nevertheless, EG affected the mechanical strengths of the foams negatively. Chen et al. [9] used a mixture of liquid macromolecular nitrogen–phosphorous compound (CPIFR) and EG to treat flame retardant EPS beads directly and found that the modified EPS foam with 20% CPIFR and 10% EG has good flame retardancy (LOI 33.9%, UL94-V0).

Polymer nanocomposites have aroused a great attention in the past two decades. Nano-scaled fillers not only improve mechanical properties [10, 11], but also reduce flammability of polymers [12]. Wang et al. [13] found that the addition of nano-ZrO_2 into the PMMA can reduce the peak heat release rate, enhance the thermal stability, and influence the carbonaceous char formation. The synergistic flame retardant effect between oxide nanoparticles (i.e., hydrophobic silica) and APP in polystyrene has been reported by Cinausero et al. [14]. Lu et al. [15] investigated the flame retardancy and thermal stability of intumescent flame-retarded polystyrene composites (PS/IFR) combined with organically modified layered inorganic materials (montmorillonite clay and zirconium phosphate), nanofiber (multiwall carbon nanotubes), nanoparticle (Fe_2O_3) or a nickel catalyst. As for nano-scaled fillers used in polymeric foams, there are some publications. For example, Ciecierska et al. [16] found that a very small addition (up to 0.05 wt%) of carbon nanotubes to rigid polyurethane foams (RPUF) can improve the mechanical strength of the PURF by about 20%, enhance the thermal stability and reduce the flammability of the foams. They also observed that carbon nanotubes do not improve the mechanical strengths of RPUF at higher loadings because of changes in the foam structure and non-uniform distribution of carbon nanotubes. It was also reported that nanoclay (non-treated montmorillonite) and nano-silica used in the flexible polyurethane foams can increase compressive strength greatly and rebound resilience when their loading is within 3%, and the foams totally collapse when the content of the nano-fillers is above 3% [17]. Song et al. [18] used carbon nanoparticles to reinforce phenolic foams and found that the compressive strength and thermal stability were improved. There are few studies on the use of nano-fillers in EPS foams, especially their combination with flame retardants.

In this work, we used phenolic resin combined with ammonium polyphosphate (APP) and nano-ZrO_2 as a flame retardant coating to treat EPS beads to study the effect of the mixture coating on flame retardant, mechanical and thermal properties of the EPS foams.

Experimental

Materials

EPS bead (size 0.9–1.2 mm) was provided by Wuxi Xingda Plastic New Material Co., China. Phenol–formaldehyde (PF) resin was bought from Shandong Shengquan Chemical Industry Co., China. Ammonium polyphosphate ($n > 1000$) was bought from Hangzhou JLS Flame Retardants Chemical Co., China. Nano-zirconia aqueous suspension dispersion (solid content of 50%) was bought from Suzhou Ugao Nanomaterials Co., China. Phosphoric acid (85 wt%) and toluene-*p*-sulfonic acid phosphate were of AR grade, bought from Sinopharm Chemical Reagent Co., China.

Preparation of EPS foams

EPS beads were first prefoamed by water vapor for 120 s, and stored at room temperature for 24 h. The treated EPS beads were mixed with phenolic resin, curing agent [phosphoric acid/toluene-*p*-sulfonic acid/water = 1:2:2 (mass ratio)] and flame retardants for 10 min. After that, the mixture was put into an aluminum mold and foamed by water vapor for 25 min. The EPS foams were removed when the mold was cooled to room temperature.

Characterization

Mechanical properties

Flexural strength of EPS foams was measured by a universal testing machine (DXLL-5000, Shanghai D&G Measure Instrument Co.) according to GB/T 20974-2014

Table 1 Formulations of pure EPS foam and flame-retarded EPS foams

Sample code	EPS beads (phr)	PF resin (phr)	Curing agent[a] (phr)	APP (phr)	Nano-ZrO_2 (phr)
E0	100	0	0	0	0
EPF	100	100	10	0	0
EA10	100	100	10	10	0
EA20	100	100	10	20	0
EA30	100	100	10	30	0
EA40	100	100	10	40	0
EAZ1	100	100	10	40	2.5
EAZ2	100	100	10	40	5
EAZ3	100	100	10	40	7.5

[a] Curing agent: m (phosphoric acid):m (toluene-*p*-sulfonic acid):m (water) = 1:2:2

(specified GB/T8812.1-2007), and the specimen dimensions were 120 mm × 25 mm × 20 mm. The load resolution and the loading rate for flexural strength were 0.1 N and 5 mm/min, respectively. Compressive strength of EPS foams was measured by CMT5105 microcomputer control electron universal testing machine (Shenzhen SANS Testing Machine Co.) according to GB/T20974-2014 (specified GB/T8813-2008), and the specimen dimensions were 20 mm × 20 mm × 20 mm. The load resolution and the loading rate for compressive strength were 0.1 N and 5 mm/min, respectively.

Thermal conductivity coefficient

Thermal conductivity coefficient was measured by a thermal conductivity tester (DHR-II, Xiangtan Xiangyang Instrument Co.); the load resolution of the instrument was 0.0001 W m^{-1} K^{-1} and the specimen dimensions were 100 mm × 100 mm × 10 mm.

LOI and UL-94 vertical burning test

Limited oxygen index (LOI) was measured by a HC-2 oxygen index testing apparatus (Jiangning Analysis Instrument Co.) according to GB/T2406-2009, and the specimen dimensions were 100 mm × 10 mm × 10 mm. Vertical flame test was measured in CZF-3 vertical combustion UL-94 apparatus (Jiangning Analysis Instrument Co.) according to GB/T2408-2008, and the specimen dimensions were 125 mm × 13 mm × 10 mm.

Cone calorimeter test

Cone calorimetric (CCT) tests were carried out on a FTT cone calorimeter (dual) according to the standards of ISO 5660. Each testing specimen had the dimension of 100 mm × 100 mm × 20 mm. The heat flux for the test was 35 kW/m^2.

Thermal gravimetric analysis

Thermogravimetric analysis (TGA) was examined by a Netzsch STA 449C thermal analyzer at a heating rate of 20 °C/min under nitrogen flow. The weight of all samples was about 10 mg in an Al_2O_3 pan and heated from room temperature to 800 °C.

X-ray photoelectron spectroscopy and X-ray diffraction analysis

X-ray photoelectron spectroscopy (XPS) was recorded with Thermo Scientific ESCALAB 250Xi to investigate the elemental content and the chemical combinations of the chars after the cone calorimeter test. X-Ray diffraction (XRD) was recorded by RigakuD/max2550VB3+/PC to investigate the compositions of the chars after the cone calorimeter test in the range of 5°–80°, and the scanning rate was 5° min^{-1}.

Results and discussion

Mechanical properties and thermal insulation

Table 1 presents the formulations of pure EPS foam and the treated EPS foams obtained from the coated EPS beads by phenolic resin (PF), the mixture of PF resin and the flame retardant (APP), and the mixture of PF resin, APP and nano-ZrO_2. Mechanical properties of pure EPS foam and the treated EPS foams were investigated, and the results are listed in Fig. 1. It can be seen that the compressive strength and flexural strength of pure EPS foams (sample E0) are 0.33 and 0.63 MPa, respectively. The coating of phenolic resin on the surface of EPS beads results in 18% increase in compressive strength and 13% increase in flexural strength of the treated EPS foam (sample EPF) compared with pure EPS foam (sample E0). The compressive strength of the EPS foams

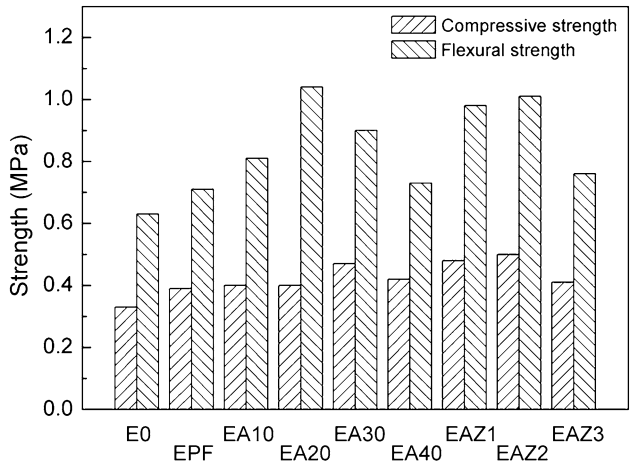

Fig. 1 Mechanical properties of pure EPS foam and flame-retarded EPS foams

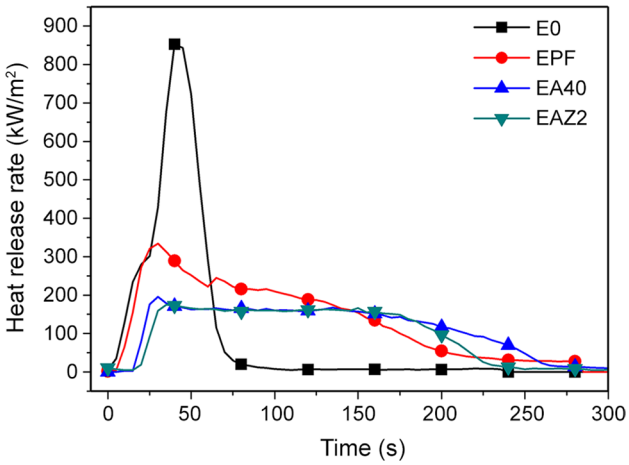

Fig. 2 Heat release rate of pure EPS foam and flame-retarded EPS foams

obtained from the coating of EPS beads by a mixture of phenolic resin and APP increases first with increasing the APP loadings, reaches a maximum at 30 phr APP (sample EA_{30}), increasing by 42% compared with pure EPS foam (sample E0), and then decreases gradually with a further increase in the loading. The effect of APP loadings on the flexural strength of the treated EPS foams is quite similar to that of compressive strength. The difference between them is that the flexural strength of the treated EPS foams reaches a maximum, at 20 phr APP (sample EA_{20}), by 65% compared with pure EPS foam (sample E0). The reason for the improvement in mechanical strengths is possibly because the mixture of PF resin and APP can be sticky toward the surface of EPS beads so as to enhance the binding force between EPS beads. The decrease in flexural and compressive strengths of the treated EPS foams with a further increase in APP loadings may be due to the fact that the mixture containing high APP loadings has a high viscosity and it is difficult to disperse the mixture on the surfaces of the EPS beads evenly.

When the mixture of PF resin and APP, containing proper amount of nano-ZrO_2, was used to treat EPS beads, the compressive and flexural strengths of the obtained EPS foams increased further compared with those of the EPS foam without nano-ZrO_2 (sample EA40). The flexural and compressive strengths of the treated EPS foamswith5 phr nano-ZrO_2 (sample EAZ2) are about 19% and by 38% higher than those of sample EA40, respectively.

As shown in Fig. 2, the thermal conductivity values of pure EPS foam and the treated EPS foams change little, and the difference among them is within the range of instrument measurement error. The results imply that the treatment on EPS beads by PF resin and the flame retardant PF resin have little influence on the thermal conductivity of the EPS foams.

Flame resistance

LOI and UL 94 ratings are commonly used to evaluate flame retardancy of polymer materials. Table 2 presents the LOI values of EPS foams and flame-retarded EPS foams. The LOI value of pure EPS foam is 19.0% indicating that it is very flammable. When the EPS beads are just coated by phenolic resin, the LOI of the obtained EPS foam increases to 22.5%. The LOI values of the flame-retarded EPS foams obtained from the coated EPS beads by the mixture of phenolic resin and the flame retardant (APP) increase gradually with the increase of APP loadings. For example, the LOI value of EA_{20} with 20 phr APP is 26.5%, and the LOI value for EA40 with 40 phr APP is 30.5%. The flame retardant systems achieve V0 rating when the APP loading reaches 40 phr.

The LOI value of the obtained EPS foams increases further when the EPS beads are coated by a mixture of phenolic resin, APP and nano-ZrO_2. The LOI value of sample EAZ2 with 40 phr APP and 5 phr nano-ZrO_2 is 31.5%, and the sample EAZ2 is able to achieve a V0 rating. The further increase of nano-ZrO_2 loading to 10 phr cannot lead to higher LOI.

Cone calorimeter has been widely used to evaluate the combustion behavior and predict the fire intensity of a material in a real fire [19]. The combustion properties of pure EPS foam (sample E0) and flame-retarded EPS foams (samples EPF, EA40 and EAZ2) were further studied by cone calorimeter test. The heat release rate (HRR) curves are presented in Fig. 2, and relative data are listed in Table 3. From the results, we can find that the peak heat release rate (PHRR) of pure EPS foam (sample E0) is 853 kW m^{-2}, and the values of sample EPF and sample EA40 are reduced by 60.8 and 77.1%, respectively. The

Table 2 Properties of pure EPS foam and flame-retarded EPS foams

Sample code	LOI (%)	UL 94 rating	Density (g cm^{-3})	Thermal conductivity (W m^{-1} K^{-1})
E0	19.0	Fail	49.0	0.0254
EPF	22.5	Fail	82.5	0.0252
EA10	24.5	Fail	82.7	0.0253
EA20	26.5	Fail	83.0	0.0253
EA30	28.0	V1	83.2	0.0252
EA40	30.5	V0	83.2	0.0254
EAZ1	31.0	V0	83.4	0.0255
EAZ2	31.5	V0	83.5	0.0248
EAZ3	31.5	V0	83.5	0.0254

Table 3 Cone calorimetric data of pure EPS foam and flame retarded EPS foams

Sample code	TTI[a] (s)	PHRR[b] (kW m^{-2})	AEHC[c] (MJ kg^{-1})	ASEA[d] (m^2 kg^{-1})	CO yield (kg kg^{-1})	CO_2 yield (kg kg^{-1})
E0	1	853	33	1109	0.078	2.13
EPF	2	334	27	728	0.070	1.82
EA40	11	195	26	770	0.099	1.64
EAZ2	15	179	14	465	0.054	0.86

[a] Time to ignition

[b] Peak heat release rate

[c] Average effective heat of combustion

[d] Average specific extinction area

PHRR value of the EPS foam with APP and nano-ZrO_2 (sample EAZ2) further decreases from 195 to 179 kW m^{-2} compared with EA40. The time to ignition (TTI) of sample E0 is 1 s, and HRR of sample E0 increases rapidly after the ignition. The TTI values of samples EPF, EA40 and EAZ2 are all higher than that of sample E0, especially the ones of samples EA40 and EAZ2. The combustion process of samples EPF, EA40 and EAZ2 are greatly prolonged compared with sample E0. The reason for the lower PHRR and the prolonged combustion process of samples EA40 and EAZ2 may be due to the fact that PF resin and APP in the foams can form good intumescent char which can prevent the heat and mass transfer between the gaseous phase and the condensed one [20]. As shown in Fig. 3, almost no char is observed after combustion of sample E0. The EPS foam treated only by the PF resin (sample EPF) produces some char, but the char is non-continuous and loose. It is clearly seen that samples EA40 and EAZ2 leave more and continuous char after the cone calorimeter test, and thus they have lower PHRR. Moreover, it can be found from Table 3 that sample EAZ2 has a lower average effective heat of combustion (AEHC) and average specific extinction area (ASEA).

From the data in Table 3, it can be seen that the CO and CO_2 yields of sample EAZ2 both decrease by 30.8% (from 0.078 to 0.054 kg kg^{-1}) and 59.6% (from 2.13 to 0.86 kg kg^{-1}), respectively, compared with E0. Besides, the average specific extinction area (ASEA) of sample EAZ2 decreases by 58.1% compared with E0 (from 1109 to 465 m^2 kg^{-1}), which indicates that the existence of nano-ZrO_2 can help to suppress smoke release of the EPS foams. The reason for the decrease in the smoke may be due to the formation of a good char by the introduction of nano-ZrO_2.

Thermal decomposition

The thermal decomposition of EPS foams was investigated by thermogravimetric analysis (TGA). Figures 4 and 5 show TGA and DTG curves of pure EPS foam (sample E0), and flame-retarded EPS foams (samples EPF, EA40 and EAZ2), and some data are listed in Table 4. It can be seen that pure EPS foam (sample E0) begins to decompose at about 100 °C, and the temperature at 5% weight loss ($T_{5\%}$) is 294 °C. The $T_{5\%}$ of EPF is lower than that of sample E0, but their $T_{50\%}$ (the temperature at 50% weight loss) values are almost same. The $T_{5\%}$ and $T_{50\%}$ values of sample EA40 are higher than those of sample EPF. Compared with sample EA40, the $T_{5\%}$ of sample EAZ2 decreases, but its $T_{50\%}$ slightly increases. Moreover, the residue of sample EAZ2 at high temperatures (above 450 °C) is much higher than that of sample EA40. The residue of sample EAZ2 at 780 °C is 19.38%, while the value of sample EA40 is 6.77%. The increase in the residue of sample EAZ2 at high temperatures is possibly because ZrO_2 can react with pyrophosphoric acid produced from thermal decomposition

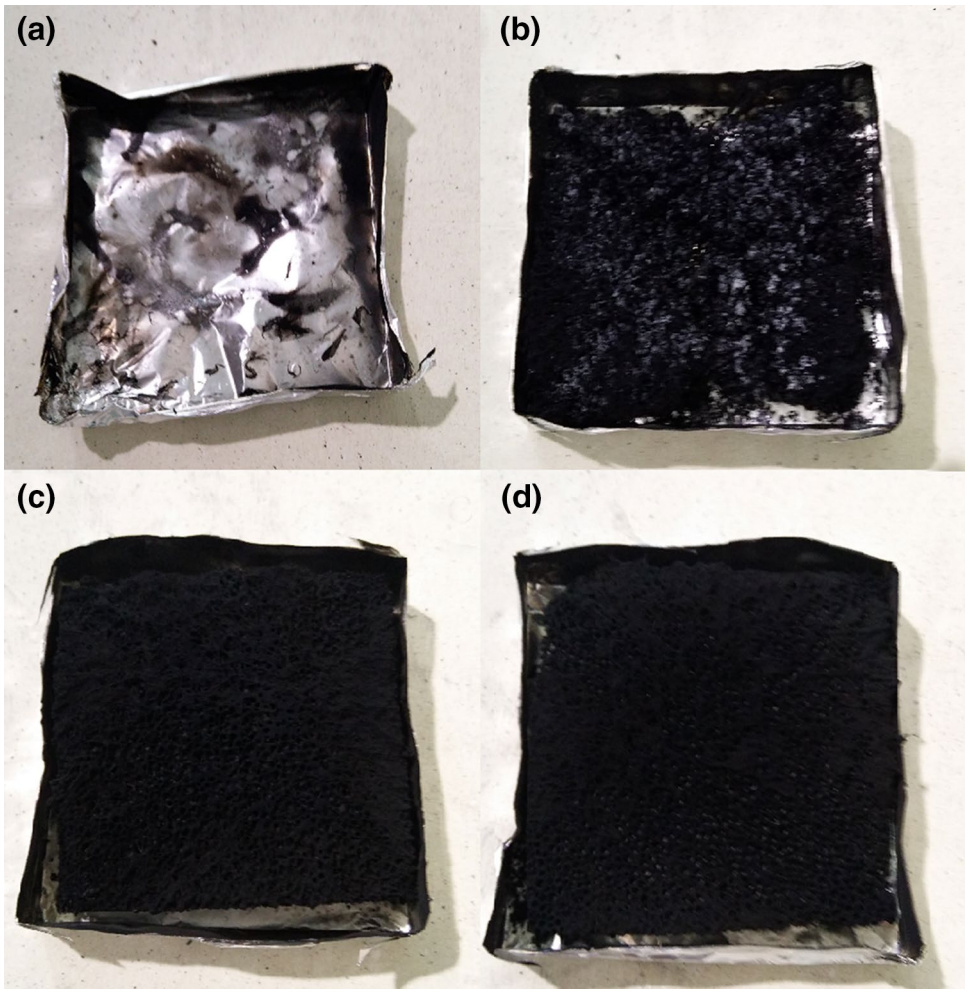

Fig. 3 The digital photos of the residual charred layer after cone calorimeter test: **a** sample E0, **b** sample EPF, **c** sample EA40, and **d** sample EAZ2

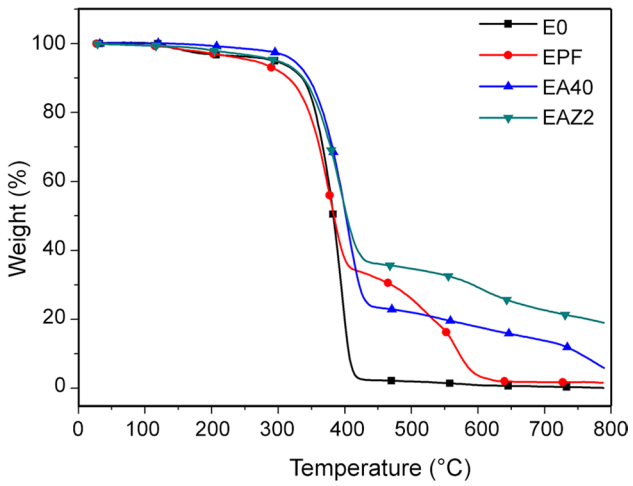

Fig. 4 TGA curves of pure EPS foam and flame-retarded EPS foams

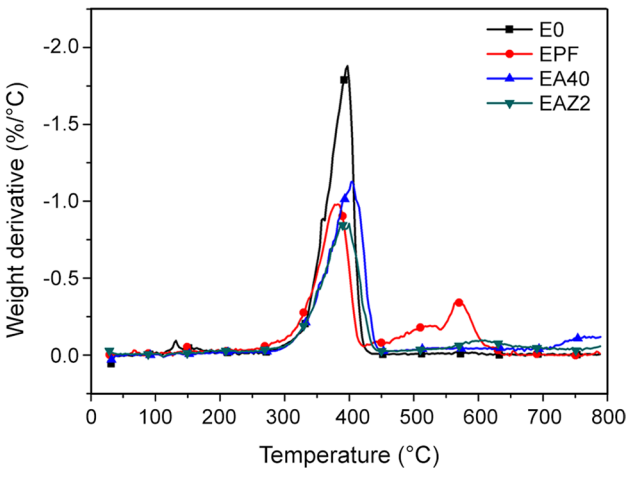

Fig. 5 DTG curves of pure EPS foam and flame-retarded EPS foams

Table 4 TGA results of pure EPS foam and flame retarded EPS foams

Sample code	$T^{a}_{5\%}$ (°C)	$T^{b}_{50\%}$ (°C)	Residue at 780 °C (wt%)
E0	294	382	0.16
EPR	264	383	1.62
EA40	322	401	6.77
EAZ2	299	403	19.38

[a] Temperature at 5% weight loss

[b] Temperature at 50% weight loss

of APP to form zirconium pyrophosphate (ZrP_2O_7), which has a high thermal stability [21]. Moreover, the ZrP_2O_7 acting as solid acid could improve the quality of the char and increase its thermal stability at high temperatures [13].

Char analysis

Figure 6 is the XRD pattern of sample EAZ2 after cone calorimeter test. The diffraction peaks (18.60°, 21.52°, 24.10°, 26.44°, 30.62°, 36.08°, 49.37° and 58.07°) match well with the (111), (200), (210), (211), (220), (311), (420) and (511) reflections of ZrP_2O_7 (JCPDS 49-1079), as in the stated order. The diffraction peaks (28.17°, 31.47° and 34.16°) are attributed to the (−111), (111) and (200) reflections of ZrO_2 (JCPDS 37-1484), respectively. Moreover, it can be assessed from the intensity diffraction peaks semi-quantitatively that Zr element exists mainly in the form of zirconium pyrophosphate (ZrP_2O_7). These results reveal the reactions between ZrO_2 and the thermal decomposition products (pyrophosphoric acid) of APP during the combustion to form ZrP_2O_7. Similar results were found in the studies of intumescent flame retardant polymers with ZrO_2 [22].

The C1s spectra of samples EA40 and EAZ2 are presented in Fig. 7 and Table 5. The optimum curve-fitting is achieved by resolving the C1s spectrum of sample EA40 into four peaks, i.e., 283.8, 284.6, 285.4 and 286.4 eV, and the C1s spectrum of sample EAZ2 into five peaks, i.e., 283.8, 284.6, 285.4, 286.4 and 288.8 eV. The peak around 283.8 eV is the contribution of bulk sp^3 carbon [23, 24]. The peak around 284.6 eV is attributed to C–H and C–C in aliphatic and aromatic species. The 285.4 eV peak may be assigned to the contribution of C–O species (ether, hydroxyl group, C–O–P in hydrocarbonated phosphate) [25]. The peaks around 286.4 and 288.8 eV may be assigned to carbonyl and carboxyl groups, respectively [26]. The ratio of C1s peak intensity of oxidized carbons to non-oxidized carbons can also be used to characterize the thermal stability of char layer [25]. The ratio of sample EAZ2 is about 0.40, which is higher than that of sample EA40 (about 0.12) indicating that the thermal stability of

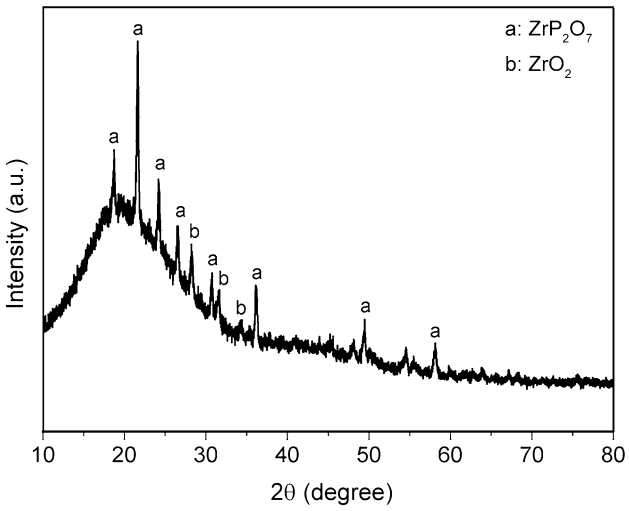

Fig. 6 XRD pattern of sample EAZ2 after cone calorimeter test

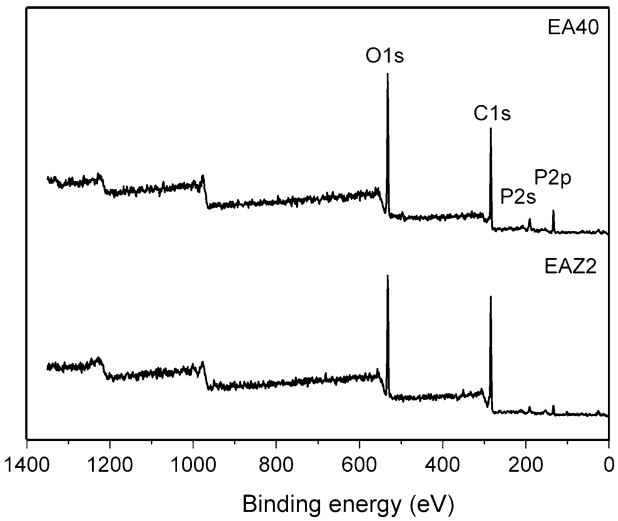

Fig. 7 C1 s spectra of the char residues

char from sample EAZ2 is enhanced compared with the one from sample EA40.

Conclusion

The mechanical properties, thermal properties and fire properties of expanded polystyrene (EPS) foams flame retarded by the combination of PF resin, APP and nano-ZrO_2, were evaluated. The compressive and flexural strengths of flame retarded EPS foam increase first with an increase in APP loadings, reach a maximum at about 30 phr APP, after that loading the values decrease compared with those of pure EPS foams. The incorporation of a small amount of nano-ZrO_2 into the APP flame- retarded

Table 5 Bending energy (eV) and content (%) of C1s spectra of the residue chars

Sample code	283.8 eV	284.6 eV	285.4 eV	286.4 eV	288.8 eV	C_O/C_{NO}
EA40	41.9%	47.7%	8.2%	2.2%	–	0.1161
EAZ2	19.4%	52.0%	15.9%	6.0%	6.7%	0.4006

C_O/C_{NO} the ratio of oxidized carbons to non-oxidized carbons

EPS foams results in an increase in flexural and compressive strengths. The LOI values of the APP flame-retarded EPS foams in presence of nano-ZrO_2 reach above 31.5%, and their UL 94 rating is V-0. The cone calorimeter results indicate that the APP flame-retarded EPS foams containing nano-ZrO_2 have lower peak heat release rate, average effective heat of combustion and average specific extinction area than those of the APP flame-retarded EPS foams without nano-ZrO_2. It is found from the thermogravimetric analysis (TGA) that the residue of the APP flame-retarded EPS foams containing nano-ZrO_2at high temperatures (above 450 °C) is much higher than that of the APP flame-retarded EPS foams. The thermal conductivity test results imply that the treatment on EPS beads by PF resin or the flame-retardant PF resin has less influence on the thermal conductivity of the EPS foams.

Acknowledgements This work was financially supported by the National Natural Science Foundation of China (No. U1205114).

References

1. Wang JQ, Chow WK (2005) A brief review on fire retardants for polymeric foams. J Appl Polym Sci 97:366–376
2. Doroudiani S, Omidian H (2010) Environmental, health and safety concerns of decorative mouldings made of expanded polystyrene in buildings. Build Environ 45:647–654
3. Levchik SV, Wei ED (2008) New developments in flame retardancy of styrene thermoplastics and foams. Polym Int 57:431–448
4. Covaci A, Gerecke AC, Law RJ, Voorspoels S, Kohler M, Heeb NV, Leslie H, Allchin CR, de Boer J (2006) Hexabromocyclododecanes (HBCDs) in the environment and humans: a review. Environ Sci Technol 40:3679–3688
5. Messer A (2010) Mini-review: polybrominated diphenyl ether (PBDE) flame retardants as potential autism risk factors. Physiol Behav 100:245–249
6. Kandola BK, Krishnan L, Ebdon JR (2014) Blends of unsaturated polyester and phenolic resins for application as fire-resistant matrices in fibre-reinforced composites: effects of added flame retardants. Polym Degrad Stabil 106:129–137
7. Hong YF, Fang XD, Yao DG (2015) Processing of composite polystyrene foam with a honeycomb structure. Polym Eng Sci 55:1494–1503
8. Hu LF, Wang ZZ (2015) Flame retardant and mechanical properties of expanded polystyrene foams containing aluminum phosphinate and expandable graphite. In: Chen S, Zhou S (eds) Proc Int Conf Adv Energy, Environ Chem Eng, vol. 23, AER-Adv Eng Res, pp 223–226
9. Chen X, Liu Y, Bai SB, Wang Q (2014) Macromolecular nitrogen-phosphorous compound/expandable graphite synchronous expansion flame retardant polystyrene foam. Polym Plast Technol Eng 53:1402–1407
10. Abadchi MR, Jalali-Arani A (2015) Synergistic effects of nanoscale polybutadiene rubber powder (PBRP) and nanoclay on the structure, dynamic mechanical and thermal properties of polypropylene (PP). Iran Polym J 24:805–813
11. Wang WT, Zhang H, Dai YY, Hou HX, Dong HZ (2015) Effects of various nanomaterials on the properties of starch/poly(vinyl alcohol) composite films formed by blow extrusion process. Iran Polym J 24:687–696
12. Morgan AB, Harris RH, Kashiwagi T, Chyall LJ, Gilman JW (2002) Flammability of polystyrene layered silicate (clay) nanocomposites: carbonaceous char formation. Fire Mater 26:247–253
13. Wang XL, Wu LH, Li J (2011) Synergistic flame retarded poly(methyl methacrylate) by nano-ZrO_2 and triphenylphosphate. J Thermal Anal Calorim 103:741–746
14. Cinausero N, Azema N, Lopez-Cuesta JM, Cochez M, Ferriol M (2011) Synergistic effect between hydrophobic oxide nanoparticles and ammonium polyphosphate on fire properties of poly(methyl methacrylate) and polystyrene. Polym Degrad Stab 96:1445–1454
15. Lu HD, Wilkie CA (2010) Study on intumescent flame retarded polystyrene composites with improved flame retardancy. Polym Degrad Stab 95:2388–2395
16. Ciecierska E, Jurczyk-Kowalska M, Bazarnik P, Gloc M, Kulesza M, Kowalski M, Krauze S, Lewandowska M (2016) Flammability, mechanical properties and structure of rigid polyurethane foams with different types of carbon reinforcing materials. Compos Struct 140:67–76
17. Javni I, Song K, Lin J, Petrovic ZS (2011) Structure and properties of flexible polyurethane foams with nano- and micro-fillers. J Cell Plast 47:357–372
18. Song SA, Chung YS, Kim SS (2014) The mechanical and thermal characteristics of phenolic foams reinforced with carbon nanoparticles. Compos Sci Technol 103:85–93
19. Xu QF, Chen LZ, Harries KA, Zhang FW, Liu Q, Feng JH (2015) Combustion and charring properties of five common constructional wood species from cone calorimeter tests. Construct Build Mater 96:416–427
20. Ma YF, Wang JF, Xu YZ, Wang CP, Chu FX (2013) Preparation and characterization of phenolic foams with eco-friendly halogen-free flame retardant. J Thermal Anal Calorim 114:1143–1151
21. Wu ZP, Shu WY, Hu YC (2007) Synergist flame retarding effect of ultrafine zinc borate on LDPE/IFR system. J Appl Polym Sci 103:3667–3674
22. Gu JW, Zhang GC, Dong SL, Zhang QY, Kong J (2007) Study on preparation and fire-retardant mechanism analysis of intumescent flame-retardant coatings. Surf Coat Technol 201:7835–7841
23. Takabayashi S, Motomitsu K, Takahagi T, Terayama A, Okamoto K, Nakatani T (2007) Qualitative analysis of a diamondlike carbon film by angle-resolved X-ray photoelectron spectroscopy. J Appl Phys 101:103542
24. Takabayashi S, Okamoto K, Shimada K, Motomitsu K, Motoyama H, Nakatani T, Sakaue H, Suzuki H, Takahagi T (2008) Chemical structural analysis of diamondlike carbon films with

different electrical resistivities by X-ray photoelectron spectroscopy. Jpn J Appl Phys 47:3376–3379
25. Li GX, Yang JF, He TS, Wu YH, Liang GZ (2008) An investigation of the thermal degradation of the intumescent coating containing MoO_3 and Fe_2O_3. Surf Coat Technol 202:3121–3128
26. Ko TH, Kuo WS, Chang YH (2001) Microstructural changes of phenolic resin during pyrolysis. J Appl Polym Sci 81:1084–1089